buildings

MDPI

Article

Enhancing the Shear Capacity of RC Beams with Web Openings in Shear Zones Using Pre-Stressed Fe-SMA Bars: Numerical Study

Mohamed Elkafrawy [1,2,3], Ahmed Khalil [1,3], Mohammad AlHamaydeh [1,3], Rami Hawileh [1,3,*] and Wael Abuzaid [1,4]

[1] Materials Science and Engineering Program, College of Arts and Sciences, American University of Sharjah, Sharjah P.O. Box 26666, United Arab Emirates; b00089515@aus.edu (M.E.); b00079152@alumni.aus.edu (A.K.); malhamaydeh@aus.edu (M.A.); wabuzaid@aus.edu (W.A.)
[2] Structural Engineering Department, Faculty of Engineering, Tanta University, Tanta P.O. Box 31733, Egypt
[3] Department of Civil Engineering, American University of Sharjah, Sharjah P.O. Box 26666, United Arab Emirates
[4] Department of Mechanical Engineering, American University of Sharjah, Sharjah P.O. Box 26666, United Arab Emirates
* Correspondence: rhaweeleh@aus.edu

Abstract: Openings in the shear span can significantly affect the structural behavior of reinforced concrete (RC) beams, particularly in terms of shear capacity and crack propagation. This paper aims to investigate the feasibility of strengthening the web opening in the shear zone of RC beams by using iron-based shape memory alloy (Fe-SMA) bars, providing valuable insights for structural engineers and researchers. Numerical analysis with ABAQUS/CAE 2020 software was employed in the current study. The research was divided into six groups of beams with web openings of different lengths (150, 300, and 450 mm), prestressing levels (0%, 30%, and 60%), and reinforcement diameters (14, 18, and 22 mm) of Fe-SMA bars. The results show that the presence of web openings can cause a significant reduction in the cracking and ultimate loads of the beams, with reductions ranging from 11% to 50% and 36% to 48%, respectively. However, by adding pre-stressed Fe-SMA bars around small web openings (100 × 150 mm), the shear capacity of the beam is restored, and the beam exhibits behavior similar to solid beams. Additionally, activating the Fe-SMA bars by 30% and 60% resulted in almost similar cracking loads but improved load-carrying capacity of the beam with small openings by 12% and 9%, respectively, compared to the solid beam. The technique proposed for enhancing shear strength is most effective for beams with small (100 × 150 mm) and medium (100 × 300 mm) web openings as it can restore both the beam's shear strength and stiffness. However, for beams with larger web openings (100 × 450 mm), the use of activated Fe-SMA beams can recover almost 90% of the solid beam's shear capacity. Furthermore, reinforcing small openings with Fe-SMA bars of different diameters enhances beam shear capacity and stiffness, while for larger openings, higher Fe-SMA reinforcement ratios could potentially restore the beam's full strength and stiffness. This study emphasizes the importance of strengthening web openings in RC beams, particularly in shear zones, and provides significant insights into how to strengthen beams with web openings, thereby contributing to developing safer structures. However, further laboratory experiments are recommended to validate, complement and extend the findings of this numerical study.

Keywords: Fe-SMA; RC beams; opening; shear strength; strengthening

Citation: Elkafrawy, M.; Khalil, A.; AlHamaydeh, M.; Hawileh, R.; Abuzaid, W. Enhancing the Shear Capacity of RC Beams with Web Openings in Shear Zones Using Pre-Stressed Fe-SMA Bars: Numerical Study. *Buildings* **2023**, *13*, 1505. https://doi.org/10.3390/buildings13061505

Academic Editor: Marco Di Ludovico

Received: 3 May 2023
Revised: 2 June 2023
Accepted: 6 June 2023
Published: 11 June 2023

1. Introduction

Reinforced concrete (RC) beams with openings can be found in various structures such as buildings, bridges, and tunnels. The openings are typically created to accommodate utility lines, ducts, or other mechanical equipment [1]. Architectural engineers often prefer

to avoid passing utilities such as pipes and cables under RC beams as it increases the floor height and, accordingly the building height [2]. Therefore, structural engineers had to take such openings into consideration in the preliminary design stages. The size and location of the opening significantly affect the structural behavior of RC beams. Numerous studies have been conducted on RC beams with different opening shapes, sizes, and locations [3–11]. They reported that openings in the shear zone reduce RC beams' stiffness and load-carrying capacity more than that in the flexure zone. Moreover, large openings deteriorate the beam, especially in the service stage, more than small openings [12]. Web openings could be executed in several shapes, such as circular, diamond, triangular, rectangular, etc. [13].

Plenty of studies reported different classifications of web openings in RC beams in terms of size, shape, location, and execution time [6]. Somes et al. considered the circular opening as "large" when its diameter exceeds 25% of the total beam depth [14]. Another classification criterion mentioned by Mansur suggested considering the rectangular opening as large if its length exceeds the top and bottom chord members' thicknesses [15]. Mansur's classification was based on forming four plastic hinges at each opening corner as the beam mechanism. However, Ahmed et al. recommended not categorizing the opening according to its size but the overall behavior of the beam [16]. In other words, if the beam with an opening follows the traditional theory of RC beams, then the opening could be categorized as "small." With regard to the execution time of the opening, it is better to have a pre-planned opening rather than a post-planned one. The pre-planned openings could be considered during the design stage, saving much time and cost for strengthening. Even though no specific standards or codes provide the design guidelines for such beams with openings, the design engineer could find helpful information and guidance in some design books, such as in the work by Mansur and Tan [17]. However, in some cases, post-planned openings are required after building execution for some changes in mechanical and electrical services. Hence, in such cases, strengthening RC beams is needed.

In general, strengthening of RC beams becomes necessary in some cases due to various reasons such as aging, structural damage, introducing an opening, increased loading, and changes in usage [18–20]. The significance of strengthening RC beams lies in the ability to maintain the structural integrity of a building or structure, ensuring it remains safe and stable for its intended purpose [21–23]. RC beams can be strengthened using various techniques, and the most appropriate method depends on the specific conditions and requirements of the structure [24]. To date, several researchers investigated different strengthening techniques in order to mitigate the deterioration that occurred due to the presence of openings in RC beams. For instance, Alyaseen et al. studied the effect of using Carbon Fiber-Reinforced Polymer (CFRP) sheets around the opening in shear zones [25]. They concluded that strengthening the bottom chord using one CFRP sheet in the shear zone is more beneficial than adding two CFRP layers around the chord. Chin et al. tested five beams with large circular, and rectangular openings strengthened with CFRP laminates under four-point loading [19]. The experimental results exhibited the ability of CFRP laminates to enhance the cracking and the deflection at service stages in addition to increasing the load-carrying capacity of the test beams. Hassan et al. restored the shear capacity of RC beams with a web opening in the shear zone by adding a thin layer of precast strain-hardening cementitious composites (SHCC) plate [13]. The findings showed a significant enhancement in test beams' load-carrying capacity and ductility strengthened with reinforced SHCC plate. Many other techniques were developed to strengthen RC beams with web opening, whether located in the shear or flexure zone [20,26–30]. However, to the best of the authors' knowledge, the available literature shows a research gap in strengthening RC beams with web openings in shear zones using shape memory alloy (SMA) bars.

SMAs have unique properties, such as the ability to recover the inelastic strain upon heating or unloading, which are known as the shape memory effect (SME) and superelasticity phenomenon, respectively [31,32]. Despite the high cost of SMA reinforcement, its

unique properties and potential benefits justify its utilization in reinforcing several structural elements. Moreover, SMAs exhibit easier installation processes than other alternatives, especially for pre-stressing applications. This is attributed to the aforementioned phenomenon of recovering the inelastic strains upon heating. Therefore, different applications of SMAs have been studied in recent decades [33–38]. Azadpour et al. [33] investigated the behavior of RC continuous beams strengthened with SMA strands under cyclic loading. The experimental results showed a significant improvement in the energy absorption capacity of the test specimens due to the superelasticity effect of SMAs. Schranz et al. [39] tested RC bridge deck specimens strengthened with iron-based SMA (memory-steel) bars. They embedded the bars in a new mortar layer after removing the concrete cover. The findings emphasized Fe-SMA bars' ability to enhance the strengthened specimens' cracking, yielding, and ductility. Suhail et al. used pre-stressed SMA loops in seismic retrofitting of RC beam-column joints [40]. They reported an increase of nearly 65% and 35% in the energy dissipation and ultimate load capacities, respectively.

Finite element analysis (FEA) is an important tool used in engineering and applied sciences to simulate and analyze complex physical phenomena [25,26,41–45]. It involves the use of numerical methods to approximate the solutions of partial differential equations (PDEs) that describe the behavior of the physical system under consideration. Moreover, it enables designers and engineers to optimize designs, predict performance, reduce costs, conduct research, and ensure safety and reliability [46,47]. The authors identified a research gap in strengthening RC beams with web openings in shear zones using Fe-SMA bars despite extensive literature on RC beam strengthening. This study aims to fill the gap by providing valuable insights, numerical data, and practical guidelines for utilizing Fe-SMA bars in RC beams with web openings in shear zones. The authors adopt the nonlinear finite element package ABAQUS to numerically analyze RC beams with web openings in shear zones strengthened with pre-stressed Fe-SMA bars. First, validation models are established and compared with experimental results from published test data carried out by Shahverdi et al. [48]. The numerical results are displayed in terms of crack patterns, load-deflection responses, ultimate loads, and corresponding deflections. The authors have reported the validation results in their previous study [49].

2. Finite Element Modeling (FEM)

FEM is an efficient and cost-effective alternative to laboratory tests for studying concrete structures [50]. In contrast, laboratory tests are time-consuming and costly. Nevertheless, to the best of the authors' knowledge, only a limited number of numerical studies have been conducted on RC beams with strengthened web openings. Therefore, this study aims to use the FEM to simulate the behavior of reinforced concrete beams with Fe-SMA-strengthened web openings. An overview of the constitutive models for concrete, steel, and Fe-SMA bars is presented in this section. Additionally, this section presents element types, convergence criteria, and the parametric study program. ABAQUS software with "Standard" solver is adopted in the current study [51]. This is the default solver in ABAQUS and is suitable for linear and nonlinear static analyses. It uses an implicit integration scheme to solve the equations of motion.

2.1. Material Constitutive Models

2.1.1. Concrete

ABAQUS provides several options for modeling the behavior of concrete in finite element simulations [51]. The most common types of concrete constitutive models in ABAQUS are: smeared cracking, brittle cracking, and concrete damaged plasticity [52]. The smeared cracking technique considers the concrete as a homogenous material and the cracks are not explicitly modeled. This approach is appropriate for modeling concrete structures in which cracking does not play a dominant role. On the other hand, in the brittle cracking approach, the concrete is considered as a discrete material and the cracks are explicitly modeled. This approach is suitable for modeling brittle materials where

failure occurs at a very low strain level. The last technique is Concrete Damaged Plasticity (CDP) model. This approach combines the features of the smeared cracking and brittle cracking models. The concrete is modeled as a continuous material and the cracking behavior is represented by damage variables that evolve as the concrete undergoes loading. The damage variable is used to reduce the stiffness of the concrete after cracking; it also influences the material behavior after cracking (Figure 1). In addition, the model includes a plasticity component that allows the concrete to undergo inelastic deformation before failure. This approach is suitable for modeling concrete structures where both cracking and plastic deformation are significant factors, as in RC beams. These models have different levels of complexity and assumptions, and the choice of the most appropriate model depends on the specific problem being simulated and the available experimental data [53]. Moreover, CDP model can effectively capture the behavior of different elements, such as masonry structures [54,55].

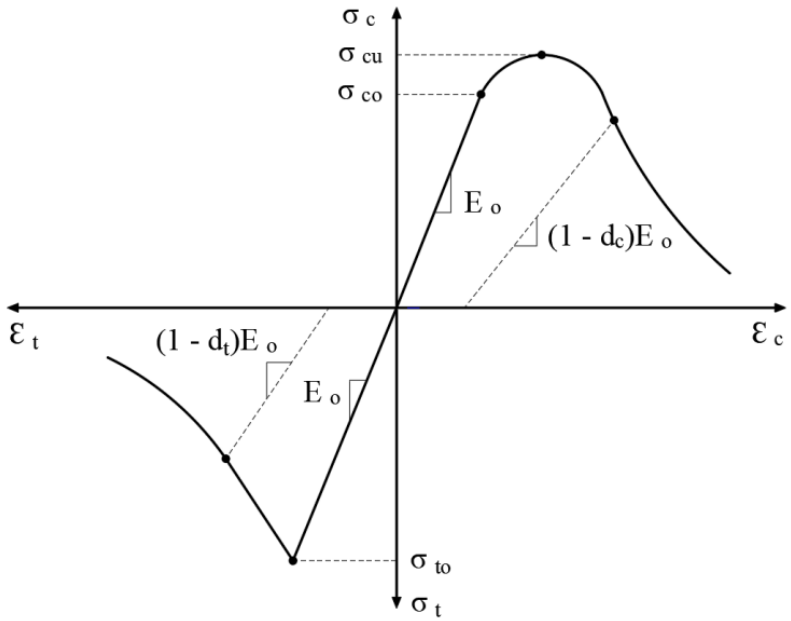

Figure 1. Schematic of concrete response to uniaxial compression and tensile loadings.

The current study adopts the CDP to model the concrete parts. In general, the stress–strain relationship of concrete in ABAQUS can be defined using material properties such as the modulus of elasticity, Poisson's ratio, yield strength, and ultimate strength. Moreover, it needs parameters specific to the chosen model, such as the concrete damage plasticity parameters defined in Table 1. These parameters are defined in the material library, which can be accessed through the ABAQUS/CAE interface or input files [49,56]. Only a few of these values were selected in the current study based on recommendations from several studies, while the remaining values are based on a sensitivity analysis conducted by the authors [49]. According to the literature, several studies proposed different concrete stress–strain relationships [57,58]. This study adopts the stress–strain relationship defined by Hsu and Hsu [58], as demonstrated in Table 2. Hsu and Hsu stress–strain relationship was chosen due to its simplicity, compatibility with experimental data, and ability to accurately represent the mechanical behavior of the concrete, making it widely used in engineering applications [49].

Table 1. Concrete damage plasticity parameters [49].

φ	e	f_{b0}/f_{c0}	K	μ
55	0.1	1.16	0.67	0.0001

where φ is the dilation angle, e is the eccentricity, f_{b0}/f_{c0} is the ratio of the initial equibiaxial to uniaxial concrete compressive strength, K is the shape parameter, and μ is the viscosity parameter.

Table 2. Compressive stress–strain relationships proposed by Hsu and Hsu [58].

Relationships	Output Parameter	Units
$\eta = \frac{n\beta x}{n\beta - 1 + x^{n\beta}} \ \ for\ 0 \leq x < x_d$	Empirical stress–strain relationship	unitless
$\eta = \frac{f_c}{f'_c}$	Normalized stress	unitless
$x = \frac{\varepsilon}{\varepsilon_o}$	Normalized strain	unitless
$\beta = \frac{1}{1 - \left[\frac{f'_c}{\varepsilon_o E_i}\right]} \ for\ \beta \geq 1.0$	Shape parameter	unitless
$\varepsilon_o = 8.9 \times 10^{-5} f'_c + 2.114 \times 10^{-3}$	Peak strain	in/in
$E_{it} = 124.31 f'_c + 3283.12$	Initial tangential modulus	kip/in^2
$\beta = \left(\frac{f'_c}{9.46}\right)^3 + 2.59$	Simplified shape parameter	unitless
$n = 1.0\ for\ 0 < f'_c < 62$MPa	Descending slope parameter	unitless
$x_d = \varepsilon_{(at 0.3 f'_c)}$	Maximum strain	in/in

where η is the normalized stress, f_c and ε are the stress and strain in general, respectively, β and n are material parameters, x is the normalized strain, x_d is the strain at 0.3 f'_c, and f'_c is the concrete stress peak, ε_o is the corresponding strain to stress peak, and E_{it} is the initial tangential modulus.

Tension stiffening refers to the phenomenon in reinforced concrete structures where the concrete between the cracks of the tensioned reinforcement stiffens due to the tensile stress transfer from the reinforcing bars. This stiffening effect increases the load-carrying capacity of the concrete structure. In ABAQUS, tension stiffening can be modeled using the CDP material model. The CDP model accounts for the degradation of the concrete stiffness due to cracking and the tension stiffening effect. The model uses a scalar damage variable to track the extent of cracking in the concrete and a tension stiffening function to model the increase in stiffness due to the tensioned reinforcement. To apply tension stiffening in ABAQUS, it is necessary to define the appropriate parameters for the CDP model, including the tensile strength and the tension stiffening function. Moreover, it is available to specify the reinforcement layout and properties to simulate the interaction between the reinforcement and the concrete. Once the material and reinforcement properties have been defined, the behavior of the reinforced concrete structure under load can be simulated using ABAQUS. The model will account for the tension stiffening effect, which can significantly improve the accuracy of the analysis, particularly for structures subjected to tensile loads. The current study utilizes the definition of tension stiffening according to CEB-FIP code [59], as depicted in Table 3. However, the authors recommended minor modifications based on the conducted sensitivity analyses, as mentioned in their previous study [49].

Table 3. Tensile stress-crack opening relationships proposed by CEB-FIP code [59].

Relationships	Output Parameter	Units
$f_t = 0.33\sqrt{f'_c}$	Tensile strength	MPa
$f_1 = 0.2 f_t$	Tensile stress	MPa
$W_c = 5\frac{G_f}{f_t}$	Maximum crack opening	mm
$W_1 = \frac{G_f}{f_t}$	Crack opening	mm
$G_f = \frac{G_{f0}}{2}\left(\frac{f'_c}{10}\right)^{0.7}$	Fracture energy	N/mm
$G_{f0} = 46.9 \times 10^{-6} D^2{}_{max} - \frac{D_{max}}{2000} + 0.026$	Factor accounting for the maximum aggregate size (D_{max})	N/mm

where f_t and G_f are the concrete's tensile strength and fracture energy, respectively, f_1 is the tensile stress, G_{f0} is the factor that accounts for the maximum aggregate size (D_{max}), W_1 is the crack width at $0.2 f_t$, and W_c represents the maximum crack width.

2.1.2. Steel Bars

In ABAQUS, steel bars can be defined using a bi-linear stress–strain relationship. The material properties of steel bars are defined by an elastic modulus and yield stress of 210 GPa and 508 MPa, respectively [48]. After defining the reinforcing bar properties, a tie constraint is used to attach the reinforcing bars to the concrete or other structural elements. The tie constraint allows the user to specify the attachment points of the reinforcing bars and the stiffness of the bond between the bars and the surrounding elements. Based on the validation results mentioned in [49], full bonding interaction between steel bars and surrounding concrete is assumed through defining embedded regions. Furthermore, stirrups are specified with the same material properties as main bars, while accounting for their different diameters.

2.1.3. Fe-SMA Bars

Recently, numerous studies have been conducted to characterize Fe-SMA with tremendous potential in civil engineering structures, but their application is still early. Recent developments in alloy composition and manufacturing offer new perspectives, particularly for repairing and constructing new structures, when utilizing these Fe-SMAs as prestressing tendons. The properties of Fe-SMA, as determined by Shahverdi et al. [48] are defined in this study. The full bonding contact surface between Fe-SMA bars and concrete is defined in ABAQUS according to experiments conducted by Shahverdi et al. [48]. The chemical composition of simulated iron-based shape memory alloy (Fe-SMA) bars is Fe-17Mn-5Si-10Cr-4Ni-1(V, C) based on mass ratio. The elastic modulus of 133 GPa and Poisson's ratio of 0.30 is utilized in this study. Due to the absence of the built-in Fe-SMA models in ABAQUS, a two-step technique is used to simulate the pre-stressed Fe-SMA bars response. First, an experimental stress–strain curve from Shahverdi et al. [48] is defined in the material properties section, similar to conventional steel bars. Second, a predefined field is activated and used to define the recovery stress, which accounts for the prestressing effect. Figure 2 depicts the abovementioned stress–strain relationship, while Figure 3 exhibits the prestressing effect on the deformed shape of the beam model. It can be noticed that the defined stress–strain curve (solid-red curve) is very close to the experimental data (black-dashed curve) during the loading stage. Three prestressing levels (P_i), which indicate the percentage recovery of stress, are defined in ABAQUS. Specifically, P_i (recovery stress) of 0% (0 MPa), 30% (225 MPa), and 60% (450 MPa) are investigated in the current study.

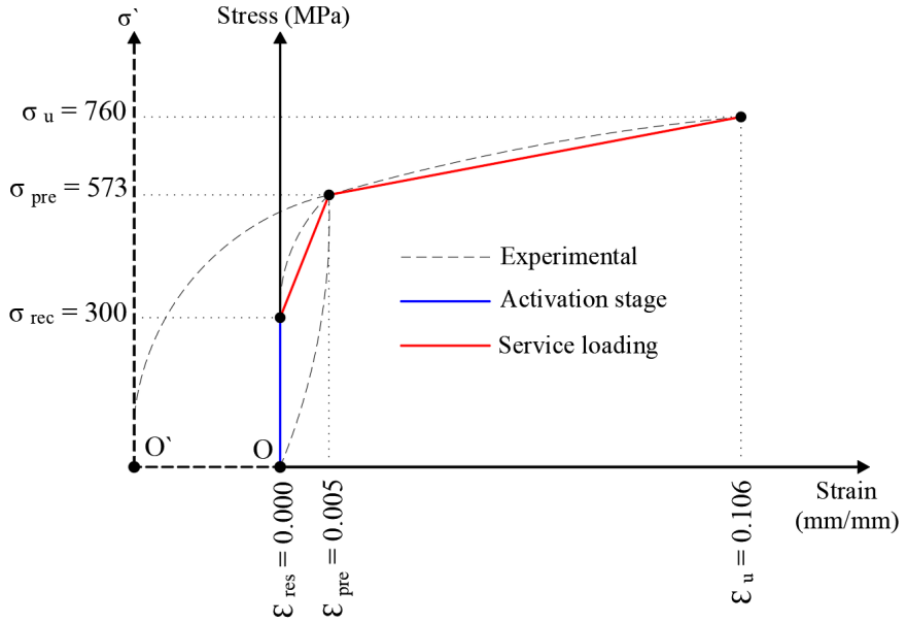

Figure 2. Stress–strain relationship of Fe-SMA in ABAQUS.

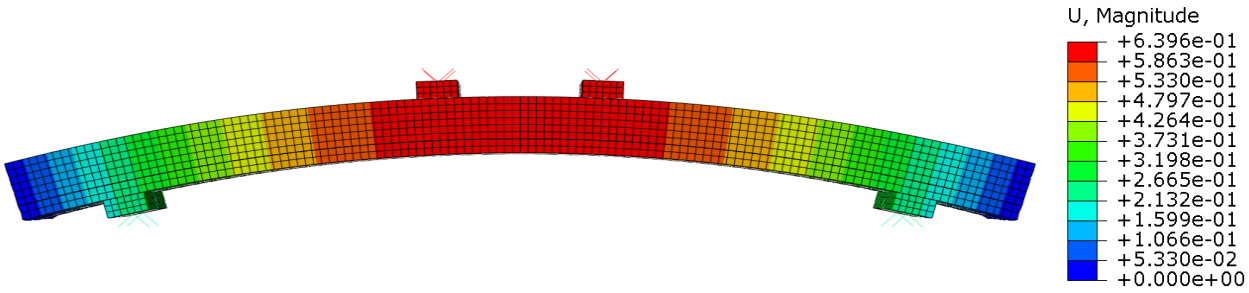

Figure 3. Prestressing effect in ABAQUS.

2.2. Element Types

The C3D8R element in ABAQUS is used to model the concrete parts, as demonstrated in Figure 4. It is a solid element with eight nodes and reduced integration (R) that is commonly used for simulating the behavior of 3D structures. This element has three degrees of freedom per node (translations in x, y, and z directions) and is suitable for modeling structures with relatively simple geometries, such as beams and columns. The reduced integration scheme in the C3D8R element reduces the number of integration points required for analysis, resulting in faster computational times. The T3D2 element is a second-order, three-node, linear displacement-based solid element used in ABAQUS for 3D simulations. It has six degrees of freedom (DOFs) per node, including three translations and three rotations. This element is utilized to define the steel and Fe-SMA bars in the current study, as shown in Figure 4. It is a popular choice for analyzing problems involving reinforcement bars with linear material behavior, such as static and dynamic structural analysis. It is also commonly used in analyzing stress concentration problems and in modeling adhesive joints.

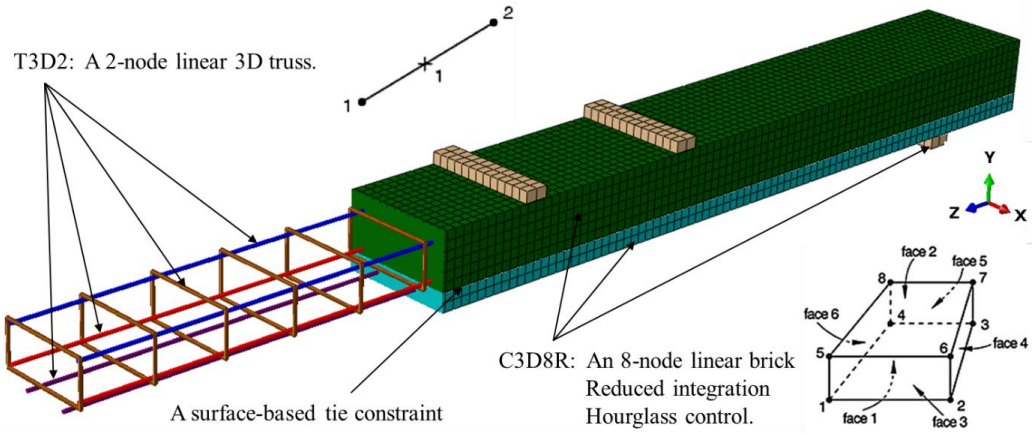

Figure 4. Element types of the validation model in ABAQUS.

In ABAQUS, mesh size can have a significant effect on the accuracy and computational efficiency of a simulation. The mesh size refers to the size of the individual elements that make up the finite element mesh used to represent the geometry of the model. Generally, using smaller element sizes (finer mesh) will improve the accuracy of the results but also increase the computational cost and time required to run the simulation. Conversely, using larger element sizes (coarser mesh) will reduce the computational cost and time required to run the simulation, but at the expense of accuracy. It is important to note that the optimal mesh size depends on the specific application and the simulation requirements. In general, a good approach is to start with a coarse mesh and gradually refine it until the results converge to a desired level of accuracy. The current study adopts a 20 mm element size to balance accuracy and computational efficiency based on a sensitivity analysis mentioned in the authors' previous study [49].

Tie constraints are used in ABAQUS to connect surfaces or edges of two or more bodies such that they move together as a single unit. The tie constraint is a type of constraint that allows the user to specify that the displacement of one surface or edge is tied to the displacement of another surface or edge. Hence, once the tie constraint has been applied, any displacement of the tied surfaces or edges will be transferred to the other connected surfaces or edges, allowing them to move together as a single unit. The surface-based tie constraint is used in the current study to connect different elements, as shown in Figure 4.

2.3. Convergence Criteria

The convergence criteria in ABAQUS are typically used to monitor the accuracy and stability of the solution during the iterative solution process. In other words, they are used to determine when the solution has converged to a sufficiently accurate and stable solution, and the iterative process can be stopped. ABAQUS provides a range of convergence criteria and allows users to customize the criteria based on the analysis type. Nevertheless, in most problems, there is no need to adjust these criteria since the default controls satisfy the desired degree of accuracy. They can vary depending on the type of analysis being performed. Some common convergence criteria used in ABAQUS include the quasi-Newton method, separated method, field equations, and constraint equations. It is worth noting that the ABAQUS default controls were used in this study, and the solution has efficiently converged.

2.4. Specimens Detailing

In the current study, the parametric study program is divided into six groups (four specimens each) in addition to a control beam, as depicted in Table 4. The cross-section dimensions of a typical beam were 350 mm in depth, 150 mm in width, and 2400 mm in total length. Beam ID specifies the opening size and Fe-SMA strengthening reinforcement for each beam. For instance, beam B-150-2T18-30% identifies a beam with an opening width of 150 mm and is strengthened using 2T18 Fe-SMA bars around the opening with 30% prestressing level. The beam is designed to fail due to shear stresses. The beams are investigated under a four-point loading scheme with a shear span of 900 mm (three times the beam depth), which assures minimal arch effect as recommended by Collins et al. [60]. The dimensions and reinforcement details of the tested beams are shown in Figure 5. The test parameters include (a) opening length, (b) Fe-SMA bars ratio, and (c) prestressing level of Fe-SMA bars. The control beam (BC) is solid without web openings and used as a benchmark for comparing the behavior of the rest of the beams with web openings. Three different opening lengths of 150, 300, and 450 mm are used in this study, maintaining a constant opening depth of 100 mm. Table 4 summarizes the characteristics of each examined beam. In group (I), four beams are modeled with opening dimensions of 100 × 150 mm: one beam without strengthening and three beams strengthened with 2T18 Fe-SMA bars at three prestressing levels (0%, 30%, and 60%). The same beam details are repeated in groups II and III but with different opening dimensions of 100 × 300 mm and 100 × 450 mm, respectively. Moreover, groups IV, V, and VI have identical opening dimensions to groups I, II, and III, respectively. However, the reinforcement ratio varies while the prestressing level is kept constant (30%).

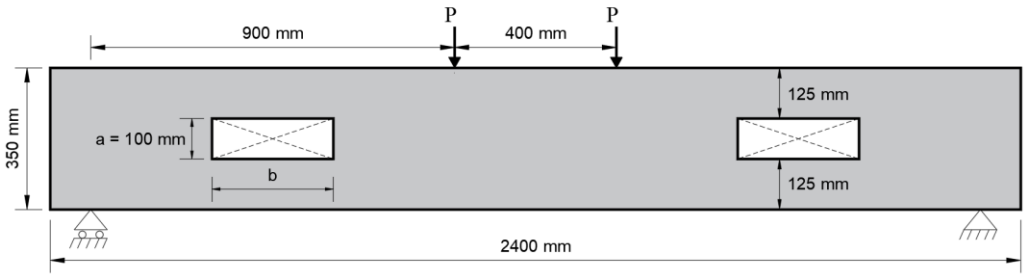

(**a**)

Figure 5. *Cont.*

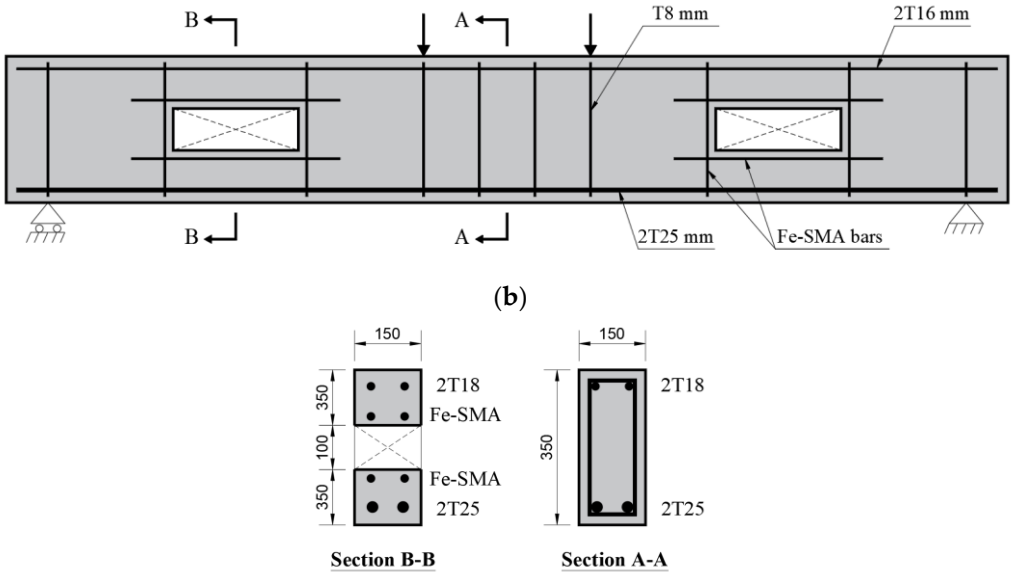

Figure 5. Details of specimens: (**a**) geometry of specimens, (**b**) details of reinforcement, and (**c**) cross-sections details.

Table 4. Parametric study program.

Group	Beam ID	Opening Dimensions		Reinf. around Opening	Reinf. Ratio (%)	Pre-Stressing Level (%)	Studied Parameter
		a (mm)	b (mm)				
Control	BC	-	-	-	-	-	-
(I)	B-150	100	150	-	-	-	Effect of pre-stressing level
	B-150-2T18-0%			2T18 mm	2.26	0	
	B-150-2T18-30%					30	
	B-150-2T18-60%					60	
(II)	B-300	100	300	-	-	-	
	B-300-2T18-0%			2T18 mm	1.13	0	
	B-300-2T18-30%					30	
	B-300-2T18-60%					60	
(III)	B-450	100	450	-	-	-	
	B-450-2T18-0%			2T18 mm	0.75	0	
	B-450-2T18-30%					30	
	B-450-2T18-60%					60	
(IV)	B-150 *	100	150	-	-	-	Effect of reinforcement ratio
	B-150-2T22-30%			2T22 mm	3.38	30	
	B-150-2T18-30% *			2T18 mm	2.26		
	B-150-2T14-30%			2T14 mm	1.37		
(V)	B-300 *	100	300	-	-	-	
	B-300-2T22-30%			2T22 mm	1.69	30	
	B-300-2T18-30% *			2T18 mm	1.13		
	B-300-2T14-30%			2T14 mm	0.68		
(VI)	B-450 *	100	450	-	-	-	
	B-450-2T22-30%			2T22 mm	1.13	30	
	B-450-2T18-30% *			2T18 mm	0.75		
	B-450-2T14-30%			2T14 mm	0.46		

a: opening height, b: opening length, *: repeated sample from a previous group.

3. Results and Discussion

3.1. Numerical Model Verification

FEM verification ensures that the FE model accurately represents the behavior of the physical system it is meant to simulate. In other words, verification is a crucial step in the FEM process as it ensures that the results obtained from the simulation are accurate and can be used with confidence. This can be done by analyzing the same structure using both the FEM model and the experimental data and comparing the results obtained from both methods. In the current study, FEM is verified by comparing the results with experimental data reported by Shahverdi et al. [48]. Shahverdi et al. [48] conducted tests and noted that the observed failure mode in all the tested beams was characterized by flexural behavior. This mode of failure entailed the steel reinforcement yielding first, followed by the subsequent crushing of the concrete under compression. The authors have validated the FEM and reported the results in their previous study. For further details, please refer to Khalil et al. [49]. To prevent unnecessary lengthening of the manuscript, the authors made a deliberate effort to avoid duplicating ideas or content that had already been presented in their previous publication. Nevertheless, for simplicity, the authors present some of the verification criteria in the current study: load-deflection behavior and cracking patterns, as shown in Figures 6 and 7, respectively. Figure 6 depicts a comparison of the load-deflection behavior results from the FEM and experiments conducted by Shahverdi et al. [48]. Beams 10 and 11 were strengthened with Fe-SMA bars embedded within a shotcrete layer attached to the soffit of the beam. The load-deflection curves based on the FEM agree reasonably well with the experimental curves. However, discernible discrepancies in the initial loading stages can be observed, primarily stemming from the inherent limitations of the numerical solution to anticipate all experimental conditions, such as the existence of initial thermal microcracks. Moreover, Figure 7 displays the cracking patterns of FEM and experiments conducted by Shahverdi et al. [48]. Hence, the verification results can be accepted in the current study, and the FEM can be trusted since the differences is almost negligible.

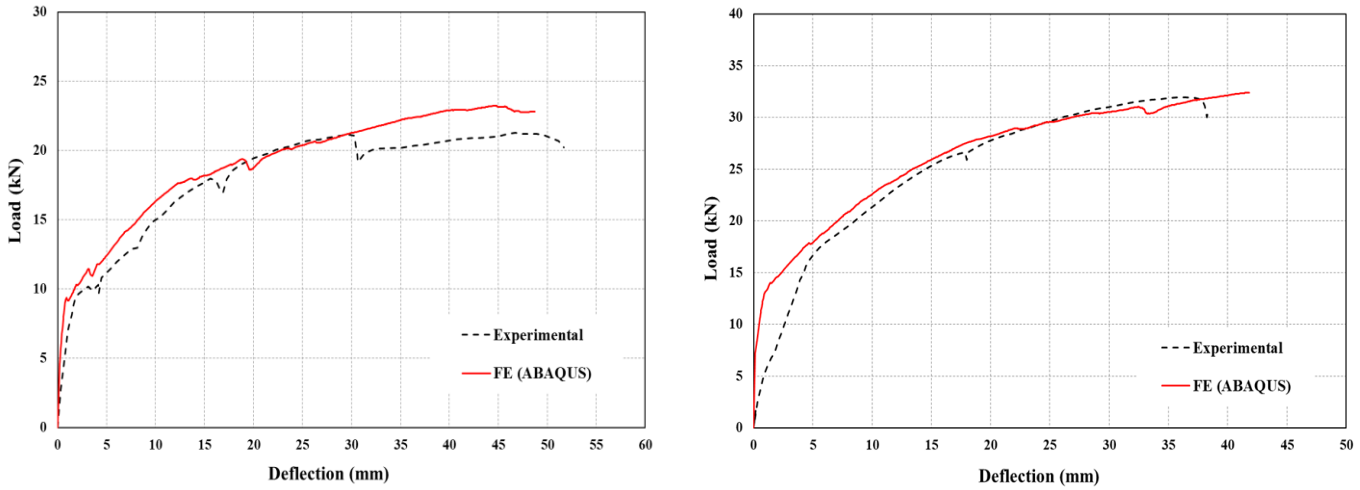

Figure 6. Load-deflection comparison of FEM and experimental results by Shahverdi et al. [48] of (**a**) beam 10 and (**b**) beam 11.

3.2. Paramteric Investigation

In RC beams, shear forces are transferred between the upper and lower portions of the beam through the concrete and the shear reinforcement. When the applied shear force becomes significant, it can cause diagonal tension stresses in the concrete along the shear plane. If the shear stress exceeds the resistance capacity of the concrete in tension, shear cracks start to develop. Several studies investigated the shear cracking in RC beams [61–63].

The presence of an opening in the shear span can alter the stress distribution and shear flow, potentially leading to changes in the development and propagation of shear cracks.

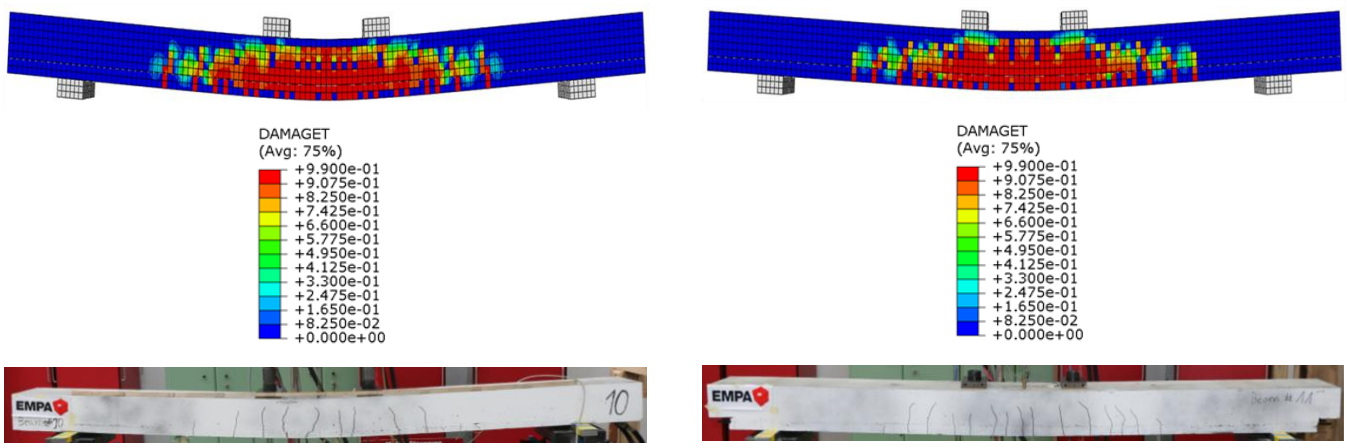

(**a**) (**b**)

Figure 7. Cracking patterns comparison of FEM and the experimental results by Shahverdi et al. [48] of (**a**) beam 10 and (**b**) beam 11.

3.2.1. Effect of Opening Size

Introducing openings in the shear span can significantly reduce the shear capacity of the beam, which can lead to structural failure. Therefore, it is essential to understand the effect of openings in the shear span of RC beams and to develop design guidelines to ensure the safe and efficient use of these beams in building construction. In this context, this topic is of significant interest to researchers and practitioners in the field of structural engineering. Figure 8 demonstrates the crack pattern of RC beams at ultimate load with different opening sizes. The occurrence of cracks, which are primarily induced by shear forces, can lead to reduced load-carrying capacity. The opening interrupts the formation of the diagonal compression strut, altering the load transfer mechanism and reducing the effectiveness of the shear reinforcement. Consequently, the beam's ultimate shear capacity is compromised, requiring additional design considerations. As shown in Figures 9 and 10, the load-carrying capacity of RC beams decreased by 37%, 36%, and 48% when openings of 150, 300, and 450 m were introduced into the shear span, respectively, compared to the control beam. Although B-150 and B-300 had almost similar ultimate loads, B-300 had a lower cracking load of around 16% and 25% compared to B-150 and BC, respectively. In contrast, the cracking load of beam B-450 decreased by 50% compared to the control beam. Importantly, the cracking load was determined by identifying the point of initial slope change in the load-deflection curve. Consequently, this study explores the feasibility of using Fe-SMA bars to restore the shear strength of RC beams with openings in the shear span, as described in the following sections.

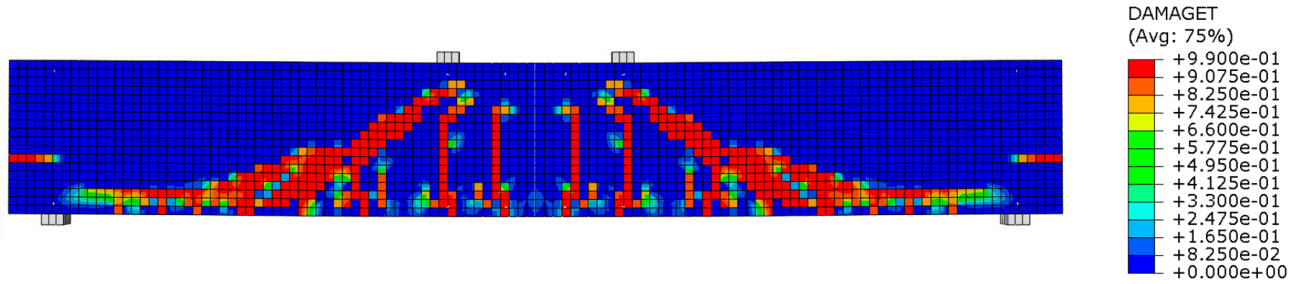

(**a**)

Figure 8. *Cont.*

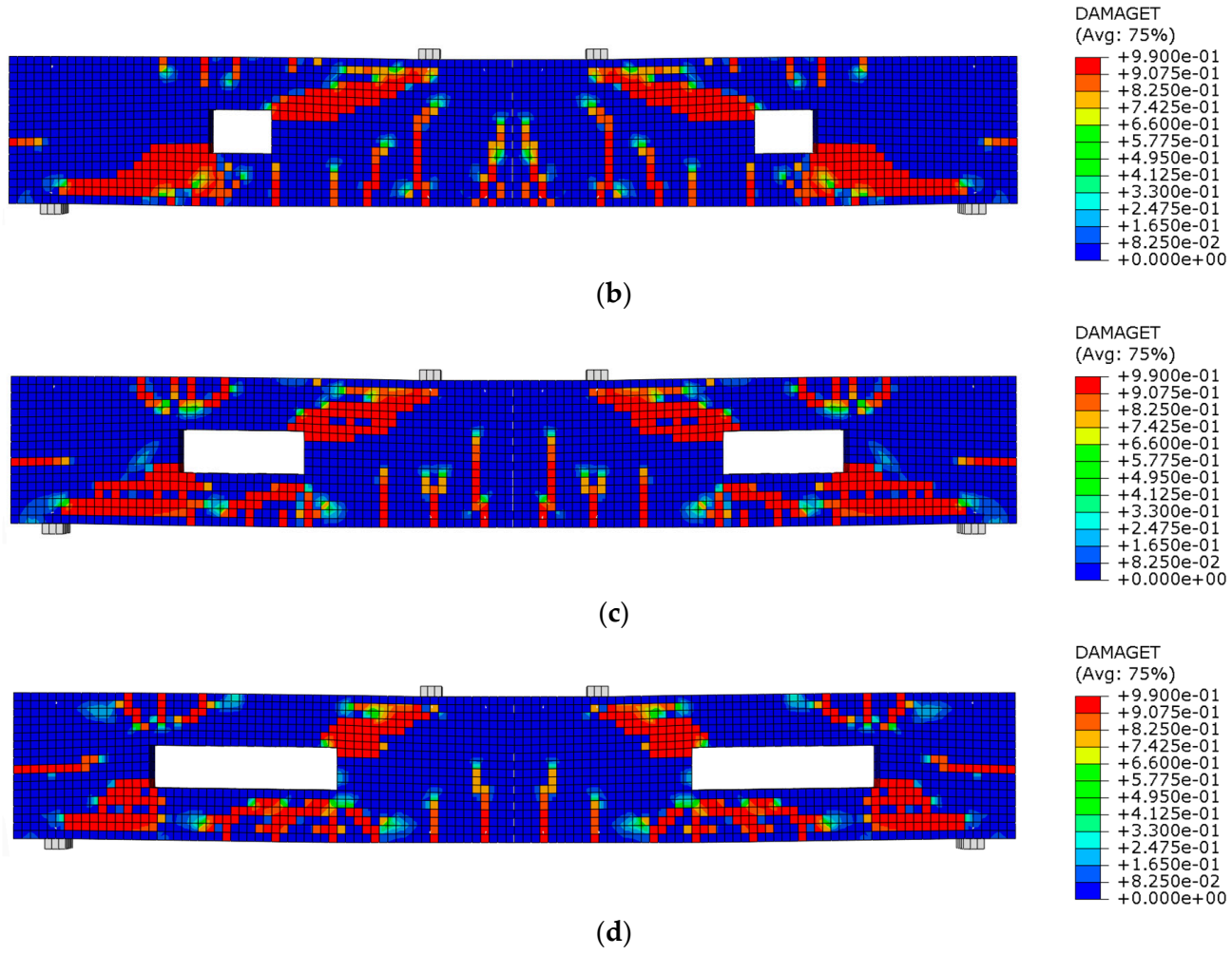

Figure 8. Effect of introducing an opening on the crack pattern. (**a**) BC. (**b**) B-150. (**c**) B-300. (**d**) B-450.

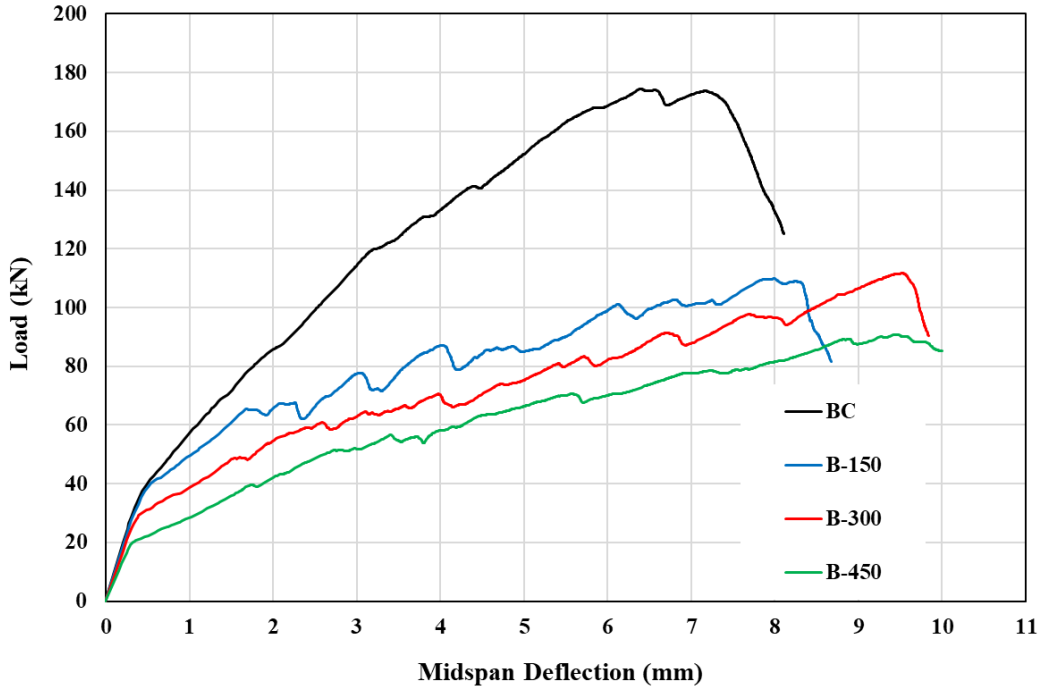

Figure 9. Effect of introducing an opening in the shear span on the load-deflection response.

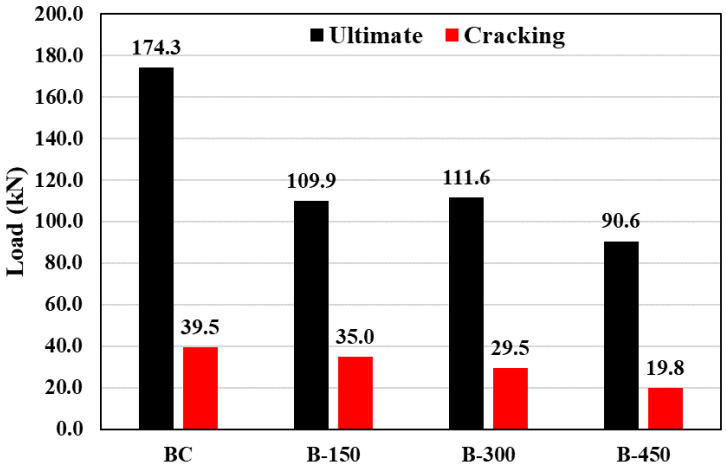

Figure 10. Effect of introducing an opening in the shear span on ultimate and cracking loads.

3.2.2. Effect of Prestressing Level

The following section delves into the impact of different prestressing levels of Fe-SMA bars around the opening on the beams' overall response. To prevent the manuscript from becoming excessively long, Figure 11 serves as an illustrative example by displaying only the cracking pattern of beams in group II. It can be noticed that the presence of the opening induces stress concentrations, leading to crack initiation near the corners of the opening. These initial cracks propagate in both vertical and diagonal directions, interacting with adjacent cracks and reinforcing bars. The crack propagation behavior depends on factors such as the opening size and prestressing level of Fe-SMA bars. Increasing the prestressing level of Fe-SMA bars in RC beams with openings offers a promising approach to mitigate crack localization and enhance structural integrity.

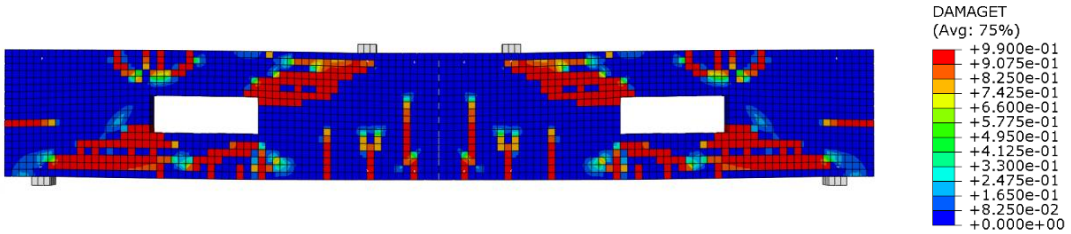

(**a**)

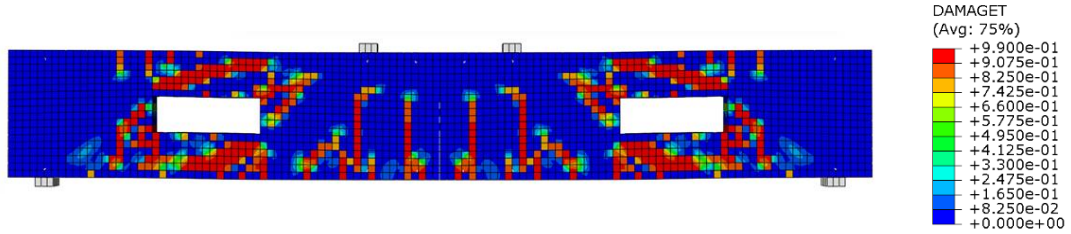

(**b**)

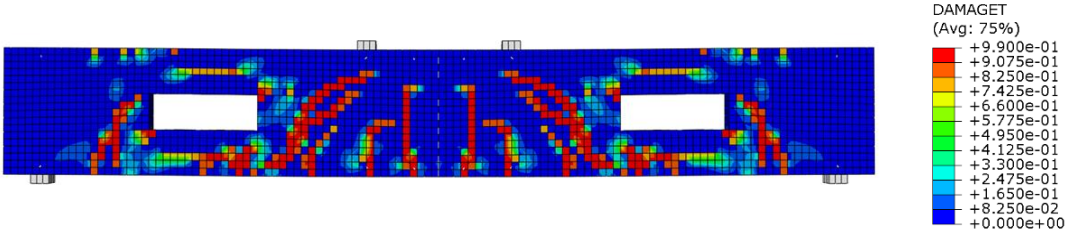

(**c**)

Figure 11. *Cont.*

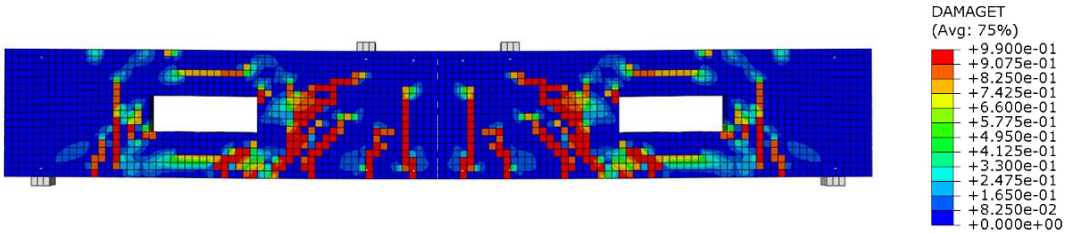

(**d**)

Figure 11. Effect of prestressing level on the crack pattern of beams in group II. (**a**) B-300. (**b**) B-300-2T18-0%. (**c**) B-300-2T18-30%. (**d**) B-300-2T18-60%.

Table 5 shows a summary of the numerical results. Moreover, in Figure 12, the load-deflection response of beams in groups I, II, and III are presented, where the difference between these groups is the opening length (150, 300, and 450 mm, respectively). The control beam (BC) achieved cracking and ultimate loads of 39.5 kN and 174.3 kN, respectively. As pointed out previously, the introduction of web openings of various lengths (150, 300, and 450 mm) significantly reduced the cracking and ultimate loads, with reductions ranging from 11% to 50% and 36% to 48%, respectively. However, when 2T18 mm Fe-SMA bars were added around the small web opening (100 × 150 mm), the shear capacity was restored, and the beam exhibited behavior similar to the solid beam (BC) with comparable ultimate load values. Additionally, activating the strengthening Fe-SMA bars by 30% and 60% resulted in almost similar cracking loads but improved the load-carrying capacity of the beam by 12% and 9%, respectively, compared to the BC beam. These results highlight the importance of strengthening web openings in RC beams, especially those in shear zones, and the effect of prestressing on crack closure. The stiffness of the beam decreased with the presence of web openings, but it can be restored and even increased by strengthening the opening with activated Fe-SMA bars, as shown in Figure 12a.

Table 5. Results summary of groups I, II, and III.

Group	Beam ID	P_{ult}, kN	P_{cr}, kN	δ_{ult}, mm	δ_{cr}, mm
Control	BC	174.3	39.5	6.38	0.39
I	B-150	109.9	35.0	8.00	0.35
	B-150-2T18-0%	171.7	35.1	6.62	0.39
	B-150-2T18-30%	196.5	35.2	5.91	0.42
	B-150-2T18-60%	190.1	35.5	5.62	0.43
II	B-300	111.6	29.5	9.52	0.38
	B-300-2T18-0%	132.7	31.2	6.94	0.39
	B-300-2T18-30%	171.3	33.6	6.19	0.43
	B-300-2T18-60%	179.2	34.5	6.20	0.48
III	B-450	90.6	19.8	9.47	0.29
	B-450-2T18-0%	119.0	28.5	7.37	0.41
	B-450-2T18-30%	148.8	32.8	9.27	0.55
	B-450-2T18-60%	167.2	33.8	8.93	0.56

Table notations: P_{ult} is the ultimate load, P_{cr} is the cracking load, δ_{ult} is the deflection at ultimate load, and δ_{cr} is the deflection at cracking load.

On the other hand, reinforcing the opening with unactivated 2T18 Fe-SMA bars had a minor positive impact on the behavior of beams with 300 mm and 450 mm opening lengths. Nevertheless, when the Fe-SMA bars were subjected to 30% and 60% prestressing levels, the shear capacity of beams with 300 mm and 450 mm opening lengths was fully and partially restored, respectively. Specifically, beams B-300-2T18-30% and B-300-2T18-60% showed similar load-deflection behavior to BC and reached capacities of 171.3 kN and 179.2 kN, respectively, which are very close to the BC capacity of 174.3 kN. On the other hand, beams B-450-2T18-30% and B-450-2T18-60% had ultimate loads of 148.8 kN

and 167.2 kN, respectively, about 14% and 4% lower than that of BC. Furthermore, it was observed that increasing the prestressing level from 30% to 60% resulted in a slight improvement in the stiffness of the beams. These findings suggest that the proposed technique for enhancing shear strength is most effective for beams with small and medium web openings (i.e., 100 × 150 mm and 100 × 300 mm), as it can restore both shear strength and stiffness. However, for beams with larger web openings of 100 × 450 mm, the use of activated Fe-SMA beams enabled recovery of almost 90% of the solid beam's shear, as demonstrated in Figure 13.

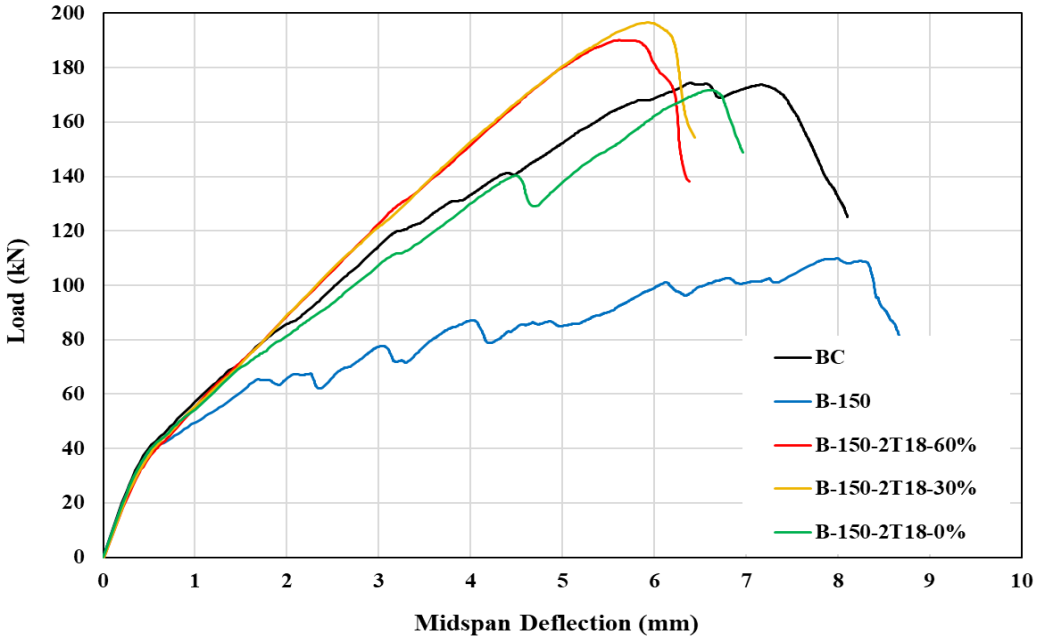

(**a**)

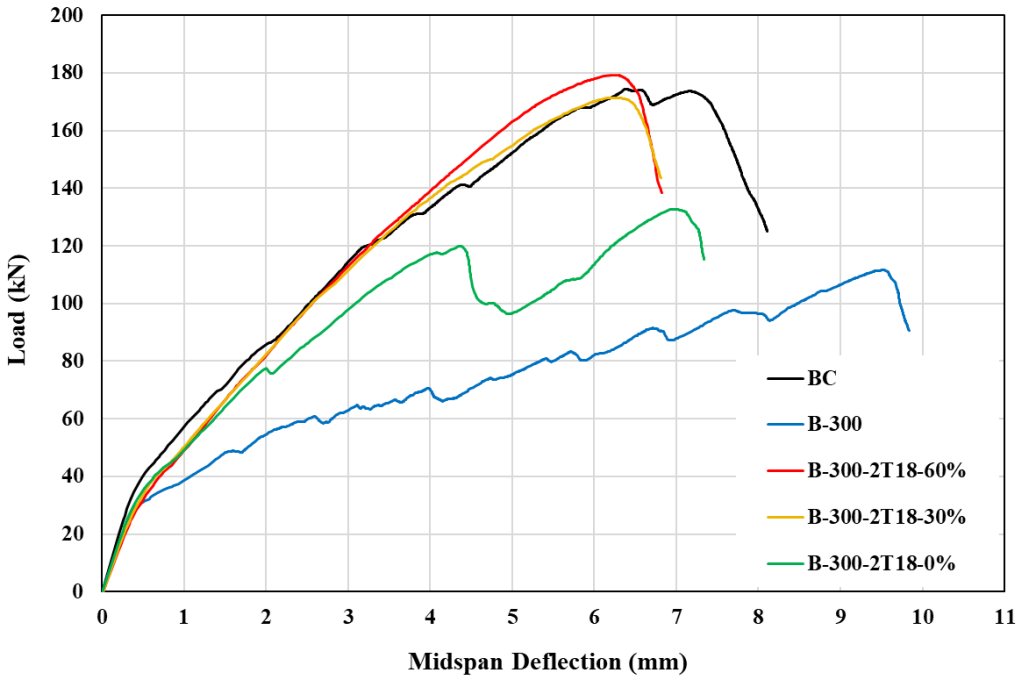

(**b**)

Figure 12. *Cont.*

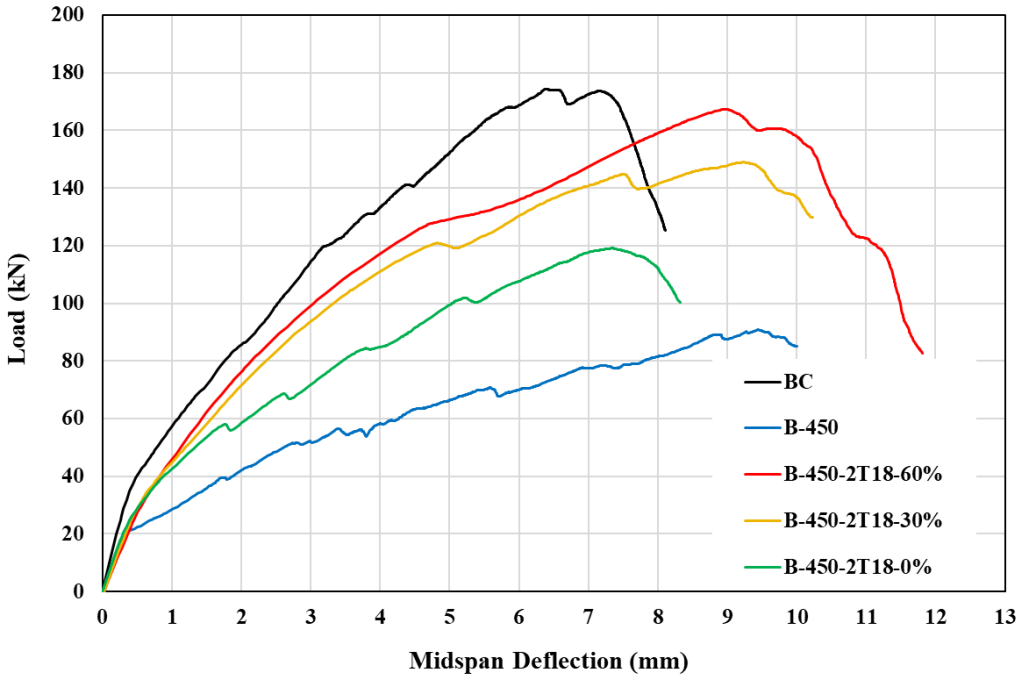

(**c**)

Figure 12. Load-deflection response for beams with web openings (**a**) group I, (**b**) group II, and (**c**) group III—Effect of pre-stressing level.

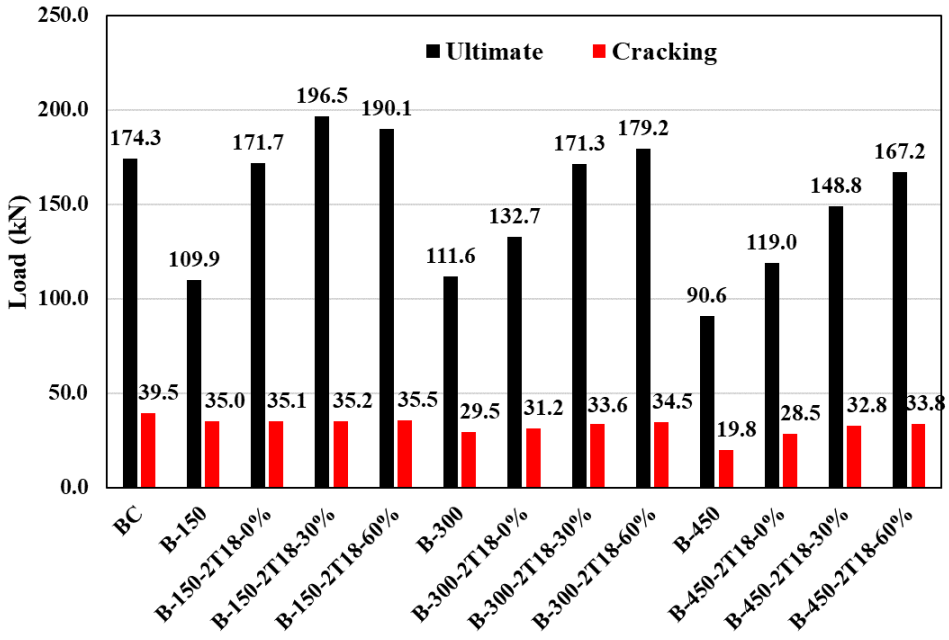

Figure 13. Ultimate and cracking loads for beams with web openings—Effect of pre-stressing level.

To conclude, the load-deflection response of RC beams with different web opening lengths showed a significant reduction in load capacity. However, the addition of activated Fe-SMA bars restored the shear capacity and increased the prestressing level, resulting in improved load-carrying capacity and stiffness. The numerical investigation conducted in this study demonstrated this approach's effectiveness in redistributing stresses and reducing crack formation around the opening. The findings provide valuable insights for optimizing the design and performance of RC beams with openings, ensuring their reliable and safe implementation in various structural applications.

3.2.3. Effect of Fe-SMA Reinforcement Ratio

This section investigates the effect of the Fe-SMA reinforcement ratio on the load-deflection response of beams with web openings. The current section examines three different Fe-SMA diameters (14, 18, and 22 mm), while keeping the prestressing level constant at 30%. The beams are split into three groups, IV, V, and VI, with varying opening lengths of 150, 300, and 450 mm, respectively. Figure 14 shows the cracking patterns for beams in group V. It can be noticed that increasing the Fe-SMA reinforcement ratio slightly mitigates crack localization in RC beams with openings. Table 6 summarizes the numerical results of groups IV, V, and VI. The findings from group IV demonstrate that reinforcing the small openings (100 × 150 mm) with Fe-SMA bars of different diameters (14, 18, and 22 mm) can enhance the beam's shear capacity and stiffness compared to the solid beam (BC), as shown in Figure 15. Similarly, using pre-stressed Fe-SMA bars to strengthen the opening area can recover the shear capacity and stiffness of a medium-sized opening beam (100 × 300 mm) compared to the BC. However, one exception was observed in group V, where the beam strengthened with 2T14 mm Fe-SMA bars exhibited a 9% lower ultimate load than the control beam, while it showed 42% higher strength than the beam with unstrengthened openings, as demonstrated in Figure 16.

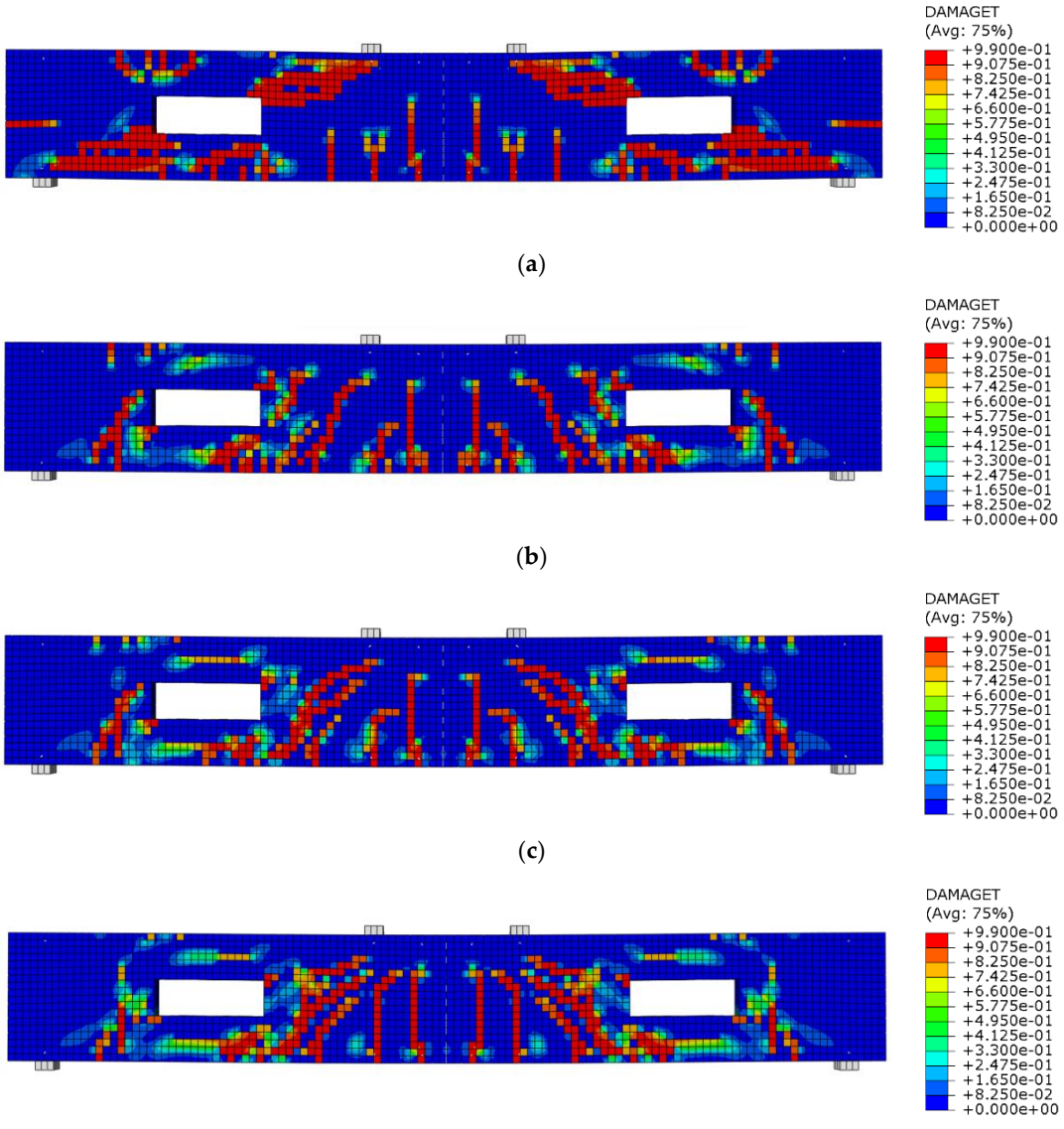

Figure 14. Effect of Fe-SMA reinforcement ratio on the crack pattern of beams in group V. (**a**) B-300. (**b**) B-300-2T14-30%. (**c**) B-300-2T18-30%. (**d**) B-300-2T22-30%.

Table 6. Results summary of groups IV, V, and VI.

Group	Beam ID	P_{ult}, kN	P_{cr}, kN	δ_{ult}, mm	δ_{cr}, mm
Control	BC	174.3	39.5	6.38	0.39
IV	B-150	109.9	35.0	8.00	0.35
	B-150-2T14-30%	192.4	35.1	6.47	0.38
	B-150-2T18-30%	196.5	35.2	5.91	0.42
	B-150-2T22-30%	182.3	35.3	5.30	0.43
V	B-300	111.6	29.5	9.52	0.38
	B-300-2T14-30%	158.5	33.3	5.61	0.42
	B-300-2T18-30%	171.3	33.6	6.19	0.43
	B-300-2T22-30%	177.9	34.1	6.38	0.45
VI	B-450	90.6	19.8	9.47	0.29
	B-450-2T14-30%	145.7	32.2	9.36	0.52
	B-450-2T18-30%	148.8	32.8	9.27	0.55
	B-450-2T22-30%	160.7	32.9	9.56	0.57

Table notations: P_{ult} is the ultimate load, P_{cr} is the cracking load, δ_{ult} is the deflection at ultimate load, and δ_{cr} is the deflection at cracking load.

On the other hand, the results from group VI indicate that reinforcing the opening area by Fe-SMA bars can significantly improve the capacity and stiffness of beams with a larger opening size (i.e., 450 mm). Nevertheless, as the opening size increased to 100 × 450 mm, neither low nor high Fe-SMA reinforcement ratios investigated in this study were able to restore the shear and ultimate strengths of the solid beam BC. This indicates that the proposed shear strengthening technique is unsuitable for restoring the beam's strength and stiffness with a large opening width (i.e., 450 mm). However, the higher reinforcement ratio showed the closest response to the solid beam in Figure 15c. Hence, it is highly recommended to investigate the feasibility of using a higher reinforcement ratio in beams with large openings in order to restore strength and stiffness, probably 2T25.

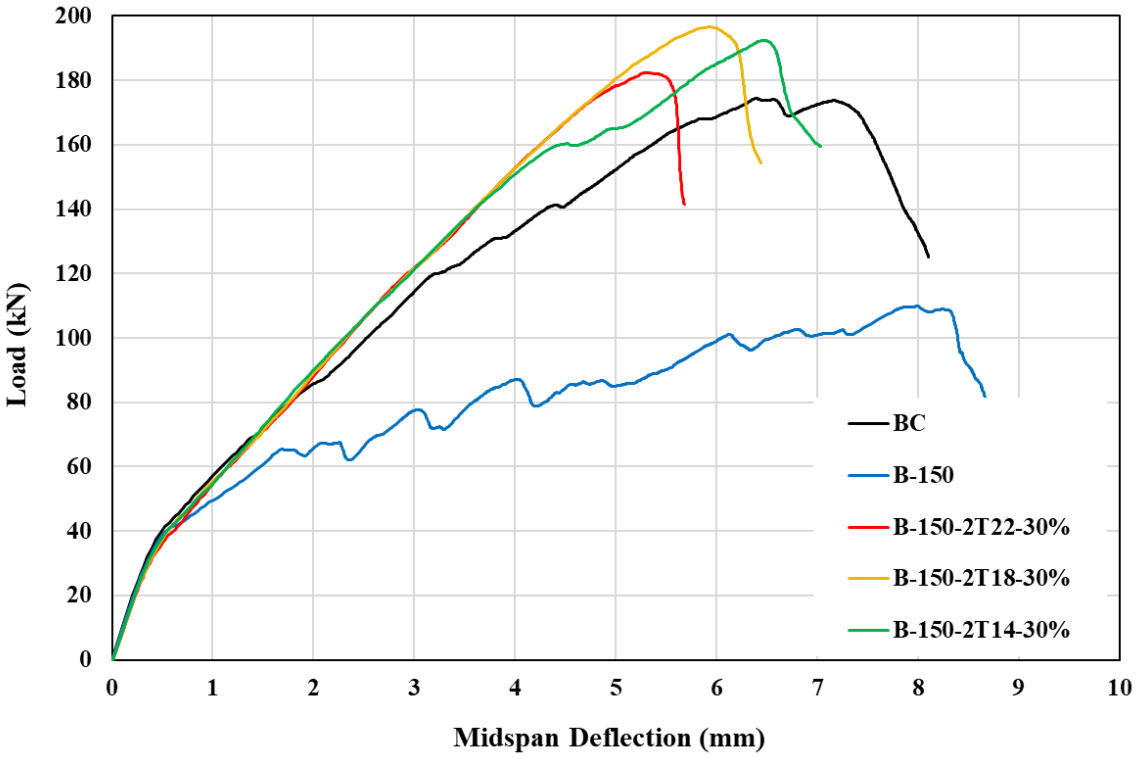

(**a**)

Figure 15. *Cont.*

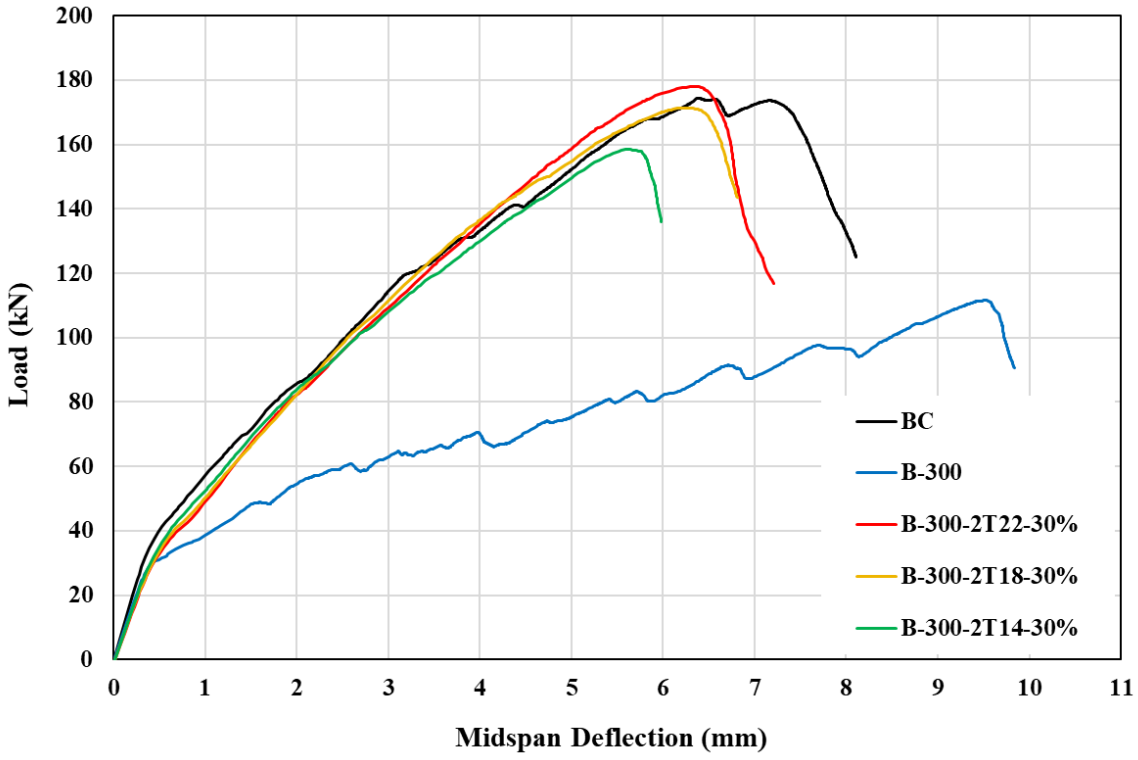

(**b**)

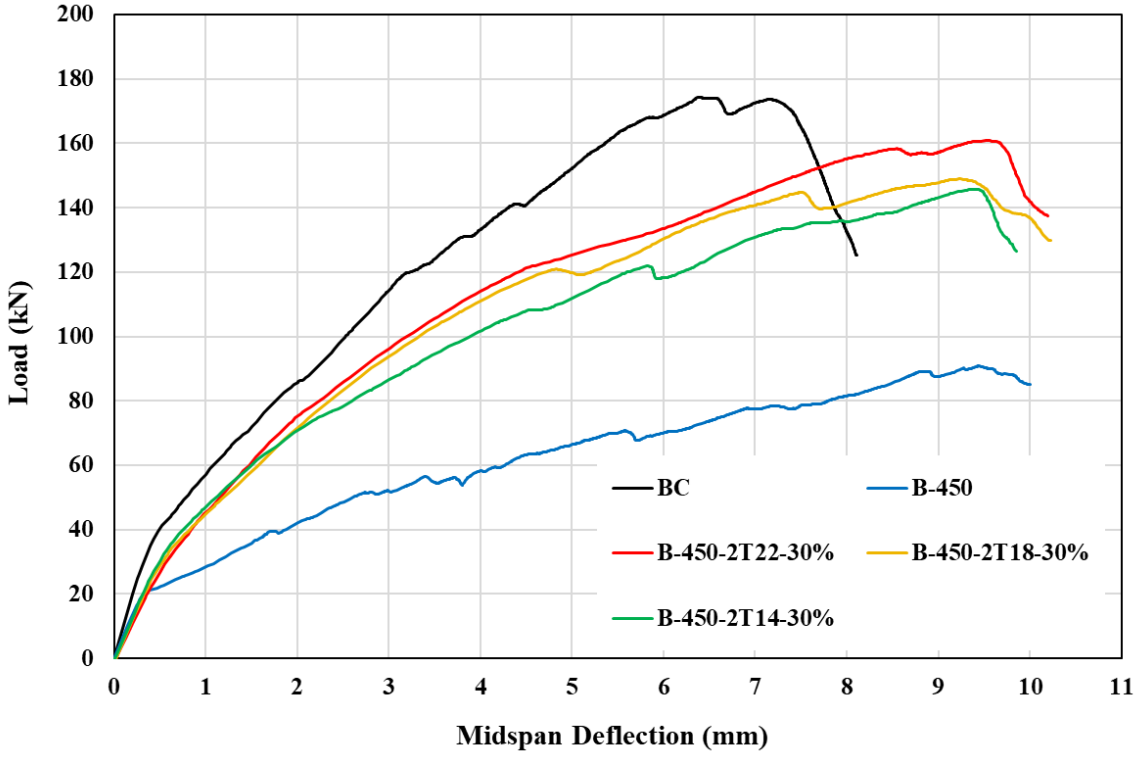

(**c**)

Figure 15. Load-deflection response for beams with web openings of (**a**) group IV, (**b**) group V, and (**c**) group VI—Effect of Fe-SMA reinforcement ratio.

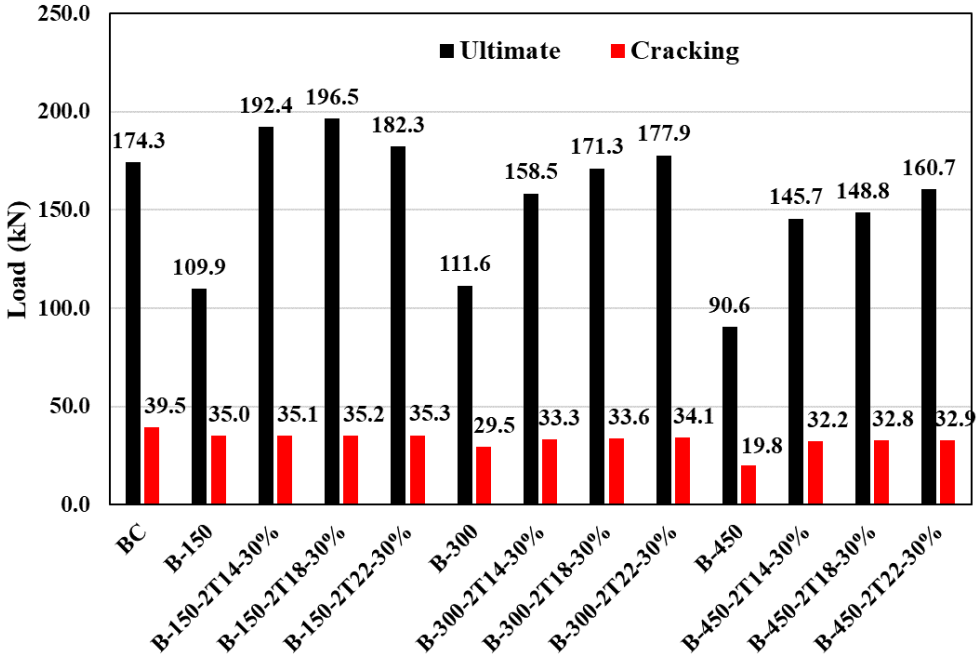

Figure 16. Ultimate and cracking loads for beams with web openings—Effect of Fe-SMA reinforcement ratio.

4. Conclusions

Reinforced concrete (RC) beams featuring shear span openings are extensively employed in diverse structural applications, owing to their improved functionality. Nevertheless, the presence of these openings can considerably impact the structural behavior of such beams, particularly with regard to shear capacity and crack propagation. This research paper examined the viability of reinforcing the web opening within the shear zone of RC beams utilizing iron-based shape memory alloy (Fe-SMA) bars, thereby offering valuable insights for researchers and structural engineers. The study employed numerical analysis conducted with ABAQUS software to accomplish this objective. Based on the numerical results of this study, the following conclusions and recommendations for future work could be drawn:

- The study investigated the effect of web openings on the load-deflection response curves of RC beams and found that the presence of openings significantly reduced the cracking and ultimate loads of the beams by up to 50 and 48%, respectively.
- Increasing either the prestressing level of Fe-SMA bars or the Fe-SMA reinforcement ratio in RC beams with openings offers a promising approach to mitigate crack localization and enhance structural integrity.
- Strengthening small-sized openings (i.e., 100 × 150 mm) with unactivated 2T18 mm Fe-SMA bars restored the beam's shear capacity and behavior to that of a solid beam (BC), with comparable ultimate and cracking load values.
- Increasing the prestressing level of the Fe-SMA bars by 30 and 60% improved the load-carrying capacity of the beams with small openings by 12% and 9%, respectively, compared to the BC beam, while almost maintaining the same cracking loads.
- The use of activated Fe-SMA bars was most effective for beams with small and medium web openings (i.e., 100 × 150 mm and 100 × 300 mm), as it could restore both the shear strength and stiffness. However, for beams with larger web openings of 100 × 450 mm, using 30 and 60% activated Fe-SMA bars enabled recovery of almost 85 and 95% of the solid beam's shear strength, respectively.
- Reinforcing small openings (100 × 150 mm) with Fe-SMA bars of different diameters (14, 18, and 22 mm) could enhance the beam's shear capacity and stiffness compared to the solid beam (BC).

- For beams with larger opening sizes (i.e., 450 mm), reinforcing the opening area with Fe-SMA bars can significantly improve the capacity and stiffness, but it still was unsuitable for restoring the full beam's strength and stiffness. Future studies could explore the feasibility of using higher Fe-SMA reinforcement ratios, such as 2T25, in beams with large openings to restore strength and stiffness.
- Overall, the findings of this study provide important insights into the impact of Fe-SMA reinforcement on the behavior of beams with web openings. These findings can help engineers and construction professionals better understand how to strengthen beams with web openings, ultimately contributing to developing safer and more ductile structures. However, it is advisable to conduct further lab experiments in order to confirm, supplement, and expand upon the results of the numerical investigation.

Author Contributions: Conceptualization, M.E. and A.K.; methodology, M.E. and A.K.; software, M.E. and A.K.; validation, M.E. and A.K.; formal analysis, M.E. and A.K.; investigation, M.E. and A.K.; resources, M.E., A.K. and W.A.; data curation, M.E. and A.K.; writing—original draft preparation, M.E. and A.K.; writing—review and editing, M.E., A.K., M.A., R.H. and W.A.; visualization, M.E. and A.K.; supervision, M.A., R.H. and W.A.; project administration, M.A., R.H. and W.A.; funding acquisition, M.A., R.H. and W.A. All authors have read and agreed to the published version of the manuscript.

Funding: This research was financially supported by the American University of Sharjah (AUS) through the Ph.D. in Material Science and Engineering (Ph.D.-MSE) Program, and the Open Access Program (OAP).

Data Availability Statement: Not applicable.

Acknowledgments: The authors greatly appreciate the financial support. This paper represents the opinions of the authors and does not mean to represent the position or opinions of the AUS.

Conflicts of Interest: The authors declare no conflict of interest.

References

1. Sayed, A.M. Numerical study using FE simulation on rectangular RC beams with vertical circular web openings in the shear zones. *Eng. Struct.* **2019**, *198*, 109471. [CrossRef]
2. Nie, X.; Zhang, S.; Chen, G.; Yu, T. Strengthening of RC beams with rectangular web openings using externally bonded FRP: Numerical simulation. *Compos. Struct.* **2020**, *248*, 112552. [CrossRef]
3. Nie, X.; Zhang, S.; Yu, T. On the FE modelling of RC beams with a fibre-reinforced polymer (FRP)-strengthened web opening. *Compos. Struct.* **2021**, *271*, 114161. [CrossRef]
4. Elsanadedy, H.M.; Al-Salloum, Y.A.; Almusallam, T.H.; Alshenawy, A.O.; Abbas, H. Experimental and numerical study on FRP-upgraded RC beams with large rectangular web openings in shear zones. *Constr. Build. Mater.* **2018**, *194*, 322–343. [CrossRef]
5. Abed, M.J.; Fayyadh, M.M.; Khaleel, O.R. Effect of web opening diameter on performance and failure mode of CFRP repaired RC beams. *Mater. Today: Proc.* **2020**, *42*, 388–398. [CrossRef]
6. Daniel, J.J. Experimental and numerical study on the cracking behavior and flexural strength of RC shallow beams with rectangular opening and varying length. *Structures* **2022**, *40*, 460–468. [CrossRef]
7. Shoeib, A.E.-K.; Sedawy, A.E.-S. Shear strength reduction due to introduced opening in loaded RC beams. *J. Build. Eng.* **2017**, *13*, 28–40. [CrossRef]
8. Mansour, W. Numerical analysis of the shear behavior of FRP-strengthened continuous RC beams having web openings. *Eng. Struct.* **2020**, *227*, 111451. [CrossRef]
9. Nie, X.; Zhang, S.; Teng, J.; Chen, G. Experimental study on RC T-section beams with an FRP-strengthened web opening. *Compos. Struct.* **2018**, *185*, 273–285. [CrossRef]
10. Nie, X.; Zhang, S.; Yu, T. Behaviour of RC beams with a fibre-reinforced polymer (FRP)-strengthened web opening. *Compos. Struct.* **2020**, *252*, 112684. [CrossRef]
11. Nie, X.; Zhang, S.; Teng, J. Strengths of RC beams with a fibre-reinforced polymer (FRP)-strengthened web opening. *Compos. Struct.* **2021**, *258*, 113380. [CrossRef]
12. Elansary, A.A.; Aty, A.A.A.; Abdalla, H.A.; Zawam, M. Shear behavior of reinforced concrete beams with web opening near supports. *Structures* **2022**, *37*, 1033–1041. [CrossRef]
13. Hassan, A.; Atta, A.M.; El-Shafiey, T.F. Restoration of the shear capacity for RC beams with web openings using precast SHCC plates. *Structures* **2020**, *25*, 603–612. [CrossRef]

14. Somes, N.F.; Corley, W.G. *Circular Openings in Webs of Continuous Beams*; American Concrete Institute, ACI Special Publiction: Farmington Hills, MI, USA, 1974; Volume SP-042, pp. 359–398.
15. Mansur, M. Effect of openings on the behaviour and strength of R/C beams in shear. *Cem. Concr. Compos.* **1998**, *20*, 477–486. [CrossRef]
16. Ahmed, A.; Fayyadh, M.; Naganathan, S.; Nasharuddin, K. Reinforced concrete beams with web openings: A state of the art review. *Mater. Des.* **2012**, *40*, 90–102. [CrossRef]
17. Mansur, M.A.; Tan, K.H. *Concrete Beams with Openings-Analysis and Design*; CRC Press LLC: Boca Raton, FL, USA, 1999.
18. Khalil, A.E.-H.; Etman, E.; Atta, A.; Essam, M. Ductility enhancement of RC beams strengthened with strain hardening cementi-tious composites. In Proceedings of the International Structural Engineering and Construction 2017, Valencia, Spain, 24–29 July 2017. [CrossRef]
19. Chin, S.C.; Shafiq, N.; Nuruddin, M.F. Strengthening of RC beams containing large opening at flexure with CFRP laminates. *Int. Sci. Index* **2011**, *5*, 1419–1425.
20. Pimanmas, A. Strengthening R/C beams with opening by externally installed FRP rods: Behavior and analysis. *Compos. Struct.* **2010**, *92*, 1957–1976. [CrossRef]
21. Khalil, A.E.-H.; Etman, E.; Atta, A.; Essam, M. Strengthening of RC beams subjected to cyclic load using ultra high-performance strain hardening cementitious composites. *Proc. Int. Struct. Eng.* **2017**, *4*, 1–6. [CrossRef]
22. El-Sisi, A.A.; El-Emam, H.M.; El-Kholy, A.E.-M.I.; Ahmad, S.S.; Sallam, H.M.; Salim, H.A. Structural Behavior of RC Beams Containing Unreinforced Drilled Openings with and without CFRP Strengthening. *Polymers* **2022**, *14*, 2034. [CrossRef]
23. Brühwiler, E.; Denarié, E. Rehabilitation and Strengthening of Concrete Structures Using Ultra-High Performance Fibre Reinforced Concrete. *Struct. Eng. Int.* **2013**, *23*, 450–457. [CrossRef]
24. Khalil, A.E.-H.; Etman, E.; Atta, A.; Essam, M. Behavior of RC beams strengthened with strain hardening cementitious composites (SHCC) subjected to monotonic and repeated loads. *Eng. Struct.* **2017**, *140*, 151–163. [CrossRef]
25. Alyaseen, A.; Poddar, A.; Alissa, J.; Alahmad, H.; Almohammed, F. Behavior of CFRP-strengthened RC beams with web openings in shear zones: Numerical simulation. *Mater. Today: Proc.* **2022**, *65*, 3229–3239. [CrossRef]
26. Altaee, M.; Cunningham, L.S.; Gillie, M. Practical Application of CFRP Strengthening to Steel Floor Beams with Web Openings: A numerical Investigation. *J. Constr. Steel Res.* **2019**, *155*, 395–408. [CrossRef]
27. El Maaddawy, T.; Sherif, S. FRP composites for shear strengthening of reinforced concrete deep beams with openings. *Compos. Struct.* **2009**, *89*, 60–69. [CrossRef]
28. Kumari, A.; Nayak, A. An experimental approach for strengthening of RC deep beams with web openings using GFRP fabrics and gas actuated fasteners. *J. Build. Eng.* **2020**, *35*, 102027. [CrossRef]
29. Hemzah, S.A.; Alyhya, W.S.; Hassan, S.A. Experimental investigation for structural behaviour of self-compacting reinforced concrete hollow beams with in-place circular openings strengthened with CFRP laminates. *Structures* **2020**, *24*, 99–106. [CrossRef]
30. Zeytinci, B.M.; Şahin, M.; Güler, M.A.; Tsavdaridis, K.D. A practical design formulation for perforated beams with openings strengthened with ring type stiffeners subject to Vierendeel actions. *J. Build. Eng.* **2021**, *43*, 102915. [CrossRef]
31. Czaderski, C.; Shahverdi, M.; Brönnimann, R.; Leinenbach, C.; Motavalli, M. Feasibility of iron-based shape memory alloy strips for prestressed strengthening of concrete structures. *Constr. Build. Mater.* **2014**, *56*, 94–105. [CrossRef]
32. Zareie, S.; Issa, A.S.; Seethaler, R.J.; Zabihollah, A. Recent advances in the applications of shape memory alloys in civil infrastructures: A review. *Structures* **2020**, *27*, 1535–1550. [CrossRef]
33. Azadpour, F.; Maghsoudi, A.; Azadpour, F.; Maghsoudi, A. Experimental and analytical investigation of continuous RC beams strengthened by SMA strands under cyclic loading. *Constr. Build. Mater.* **2019**, *239*, 117730. [CrossRef]
34. Zareie, S.; Zabihollah, A. Design and Analysis of SMA-Based Tendon for Marine Structures. In *Emerging Trends in Mechatronics*; IntechOpen: London, UK, 2020.
35. Czaderski, C.; Weber, B.; Shahverdi, M.; Motavalli, M.; Leinenbach, C.; Lee, W.; Brönnimann, R.; Michels, J. Iron-based shape memory alloys (Fe-SMA)—A new material for prestressing concrete structures. In Proceedings of the SMAR15—3rd Conference on Smart Monitoring, Assessment and Rehabilitation of Structures, Antalya, Turkey, 7–9 September 2015.
36. Wang, W.; Fang, C.; Liu, J. Large size superelastic SMA bars: Heat treatment strategy, mechanical property and seismic application. *Smart Mater. Struct.* **2016**, *25*, 075001. [CrossRef]
37. Izadi, M.; Ghafoori, E.; Shahverdi, M.; Motavalli, M.; Maalek, S. Development of an iron-based shape memory alloy (Fe-SMA) strengthening system for steel plates. *Eng. Struct.* **2018**, *174*, 433–446. [CrossRef]
38. Hong, K.N.; Lee, S.G.; Han, S.H.; Yeon, Y.M. Evaluation of Fe-Based Shape Memory Alloy (Fe-SMA) as Strengthening Material for Reinforced Concrete Structures. *Appl. Sci.* **2016**, *8*, 730. [CrossRef]
39. Schranz, B.; Michels, J.; Czaderski, C.; Motavalli, M.; Vogel, T.; Shahverdi, M. Strengthening and prestressing of bridge decks with ribbed iron-based shape memory alloy bars. *Eng. Struct.* **2021**, *241*, 112467. [CrossRef]
40. Suhail, R.; Amato, G.; Broderick, B.; Grimes, M.; McCrum, D. Efficacy of prestressed SMA diagonal loops in seismic retrofitting of non-seismically detailed RC beam-column joints. *Eng. Struct.* **2021**, *245*, 112937. [CrossRef]
41. AlHamaydeh, M.; Elkafrawy, M.; Banu, S. Seismic Performance and Cost Analysis of UHPC Tall Buildings in UAE with Ductile Coupled Shear Walls. *Materials* **2022**, *15*, 2888. [CrossRef] [PubMed]

42. AlHamaydeh, M.; Elkafrawy, M.E.; Amin, F.M.; Maky, A.M.; Mahmoudi, F. Analysis and Design of UHPC Tall Buildings in UAE with Ductile Coupled Shear Walls Lateral Load Resisting System. In Proceedings of the 2022 Advances in Science and Engineering Technology International Conferences (ASET), Dubai, United Arab Emirates, 21–24 February 2022. [CrossRef]
43. Venkatachalam, S.; Vishnuvardhan, K.; Amarapathi, G.D.; Mahesh, S.; Deepasri, M. Experimental and finite element modelling of reinforced geopolymer concrete beam. *Mater. Today Proc.* **2021**, *45*, 6500–6506. [CrossRef]
44. Behnam, H.; Kuang, J.; Samali, B. Parametric finite element analysis of RC wide beam-column connections. *Comput. Struct.* **2018**, *205*, 28–44. [CrossRef]
45. AlHamaydeh, M.; Maky, A.M.; Elkafrawy, M. INSPECT-SPSW: INelastic Seismic Performance Evaluation Computational Tool for Steel Plate Shear Wall Modeling in OpenSees. *Buildings* **2023**, *13*, 1078. [CrossRef]
46. AlHamaydeh, M.; Elkafrawy, M.E.; Aswad, N.G.; Talo, R.; Banu, S. Evaluation of UHPC Tall Buildings in UAE with Ductile Coupled Shear Walls under Seismic Loading. In Proceedings of the 2022 Advances in Science and Engineering Technology International Conferences (ASET), Dubai, United Arab Emirates, 21–24 February 2022. [CrossRef]
47. AlHamaydeh, M.; Elkafrawy, M.E.; Kyaure, M.; Elyas, M.; Uwais, F. Cost Effectiveness of UHPC Ductile Coupled Shear Walls for High-Rise Buildings in UAE Subjected to Seismic Loading. In Proceedings of the 2022 Advances in Science and Engineering Technology International Conferences (ASET), Dubai, United Arab Emirates, 21–24 February 2022. [CrossRef]
48. Shahverdi, M.; Czaderski, C.; Annen, P.; Motavalli, M. Strengthening of RC beams by iron-based shape memory alloy bars embedded in a shotcrete layer. *Eng. Struct.* **2016**, *117*, 263–273. [CrossRef]
49. Khalil, A.; Elkafrawy, M.; Abuzaid, W.; Hawileh, R.; AlHamaydeh, M. Flexural Performance of RC Beams Strengthened with Pre-Stressed Iron-Based Shape Memory Alloy (Fe-SMA) Bars: Numerical Study. *Buildings* **2022**, *12*, 2228. [CrossRef]
50. Elkafrawy, M.E.; Khalil, A.M.; Abuzaid, W.; Hawileh, R.A.; AlHamaydeh, M. Nonlinear Finite Element Analysis (NLFEA) of Pre-stressed RC Beams Reinforced with Iron-Based Shape Memory Alloy (Fe-SMA). In Proceedings of the 2022 Advances in Science and Engineering Technology International Conferences (ASET), Dubai, United Arab Emirates, 21–24 February 2022. [CrossRef]
51. Khalil, A.E.-H.; Etman, E.; Atta, A.; Essam, M. Nonlinear behavior of RC beams strengthened with strain hardening cementitious composites subjected to monotonic and cyclic loads. *Alex. Eng. J.* **2016**, *55*, 1483–1496. [CrossRef]
52. Elkafrawy, M.; Alashkar, A.; Hawileh, R.; Al Hamaydeh, M. FEA Investigation of Elastic Buckling for Functionally Graded Material (FGM) Thin Plates with Different Hole Shapes under Uniaxial Loading. *Buildings* **2022**, *12*, 802. [CrossRef]
53. Alashkar, A.; Elkafrawy, M.; Hawileh, R.; AlHamaydeh, M. Buckling Analysis of Functionally Graded Materials (FGM) Thin Plates with Various Circular Cutout Arrangements. *J. Compos. Sci.* **2022**, *6*, 277. [CrossRef]
54. Valente, M. Seismic vulnerability assessment and earthquake response of slender historical masonry bell towers in South-East Lombardia. *Eng. Fail. Anal.* **2021**, *129*, 105656. [CrossRef]
55. Milani, G.; Valente, M.; Fagone, M.; Rotunno, T.; Alessandri, C. Advanced non-linear numerical modeling of masonry groin vaults of major historical importance: St John Hospital case study in Jerusalem. *Eng. Struct.* **2019**, *194*, 458–476. [CrossRef]
56. Smith, M. *ABAQUS/Standard User's Manual, Version 6.9*; Dassault Systèmes Simulia Corp: Johnston, RI, USA, 2009.
57. Kent, D.C.; Park, R. Flexural Members with Confined Concrete. *J. Struct. Div.* **1971**, *97*, 1969–1990. [CrossRef]
58. Hsu, L.S.; Hsu, C.-T.T. Hsu1994. *Mag. Concr. Res.* **1994**, *46*, 301–312. [CrossRef]
59. Beton, C.E.-I.D. *Ceb-Fip Model Code 1990: Design Code*; Thomas Telford Publishing: London, UK, 1993.
60. Collins, M.P.; Mitchell, D. *Prestressed Concrete Structures*; Prentice Hall: Englewood Cliffs, NJ, USA, 1991.
61. Imjai, T.; Guadagnini, M.; Garcia, R.; Pilakoutas, K. A practical method for determining shear crack induced deformation in FRP RC beams. *Eng. Struct.* **2016**, *126*, 353–364. [CrossRef]
62. Hu, B.; Wu, Y.-F. Quantification of shear cracking in reinforced concrete beams. *Eng. Struct.* **2017**, *147*, 666–678. [CrossRef]
63. Setkit, M.; Leelatanon, S.; Imjai, T.; Garcia, R.; Limkatanyu, S. Prediction of Shear Strength of Reinforced Recycled Aggregate Concrete Beams without Stirrups. *Buildings* **2021**, *11*, 402. [CrossRef]